6-10-2016

Forest Soil Carbon and Nitrogen Cycles under Biomass Harvest: Stability, Transient Response, and Feedback

Anthony J. Parolari
Marquette University, anthony.parolari@marquette.edu

Amilcare Porporato
Duke University

Accepted version. *Ecological Modelling*, Vol. 329 (June 10, 2016): 64-76. DOI.

Ecological Modelling, Vol. 329 (June 10, 2016): 64-76. DOI.

Forest Soil Carbon and Nitrogen Cycles under Biomass Harvest: Stability, Transient Response, and Feedback

Anthony J. Parolari
Department of Civil and Environmental Engineering, Duke University, Durham, NC
Amilcare Porporato
Department of Civil and Environmental Engineering, Duke University, Durham, NC

Abstract

Biomass harvest generates an imbalance in forest carbon (C) and nitrogen (N) cycles and the nonlinear biogeochemical responses may have long-term consequences for soil fertility and sustainable management. We analyze these dynamics and characterize the impact of biomass harvest and N fertilization on soil biogeochemistry and ecosystem yield with an ecosystem model of intermediate complexity that couples plant and soil C and N cycles. Two harvest schemes are modeled: continuous harvest at low intensity and periodic clear-cut harvest. Continuously-harvested systems sustain N harvest at steady-state under net mineralization conditions, which depends on the C:N ratio and respiration rate of decomposers. Further, linear stability analysis reveals steady-state harvest regimes are associated with stable foci, indicating oscillations in C and N pools that decay with time after harvest. Modeled ecosystems under periodic clear-cut harvest operate in a limit-cycle with

net mineralization on average. However, when N limitation is strong, soil C–N cycling switches between net immobilization and net mineralization through time. The model predicts an optimal rotation length associated with a maximum sustainable yield (MSY) and minimum external N losses. Through non-linear plant–soil feedbacks triggered by harvest, strong N limitation promotes short periods of immobilization and mineral N retention, which alter the relation between MSY and N losses. Rotational systems use N more efficiently than continuous systems with equivalent biomass yield as immobilization protects mineral N from leaching losses. These results highlight dynamic soil C–N cycle responses to harvest strategy that influence a range of functional characteristics, including N retention, leaching, and biomass yield.

Keywords

Biomass harvest, Ecosystem nitrogen use efficiency, Maximum sustainable yield, Mineralization-immobilization, Plant–soil feedback

1. Introduction

Soil biogeochemical cycles and biomass production are closely linked processes in managed ecosystems. Soils supply plants with essential nutrients through a complex of biogeochemical processes mediated by soil organic matter (SOM) and decomposers. In turn, soil biogeochemical processes are affected by harvest management practices that determine the relative amounts of organic material (e.g., carbon (C) and nitrogen (N) ratios) and nutrients applied to the soil or harvested from the ecosystem. In particular, microbially-mediated decomposition of plant residues and associated N mineralization and immobilization fluxes control soil carbon–nitrogen (C–N) cycling and N availability after harvest (Vitousek and Matson, 1985, Prescott, 1997). Improved quantitative understanding of soil C–N cycles in response to harvest is one challenge associated with sustainable management of soil, water, and ecosystem resources (Porporato and Rodriguez-Iturbe, 2013, Porporato et al., 2015).

The coupled ecosystem C–N cycle can be understood as a complex system of plant and soil compartments linked through the dynamics of plants, SOM, and soil decomposers (Fig. 1, Fig. 2). Under management for food or timber production, harvest and associated management practices impose two changes to the structure of this dynamical system. First, management practices may take the form of an external forcing to the system, as in the export of harvested biomass or the addition of N fertilizer. Secondly, the balance of harvest export and residue application, which depends on the quality and quantity of harvested biomass, changes the plant litter flux. The plant litter flux is integral to decomposer-SOM feedback and long-term soil N availability (Vitousek and Matson, 1985, Manzoni and Porporato, 2007). In these ways, biomass harvest alters the inputs and outputs as well as the internal dynamics of ecosystem C–N cycles.

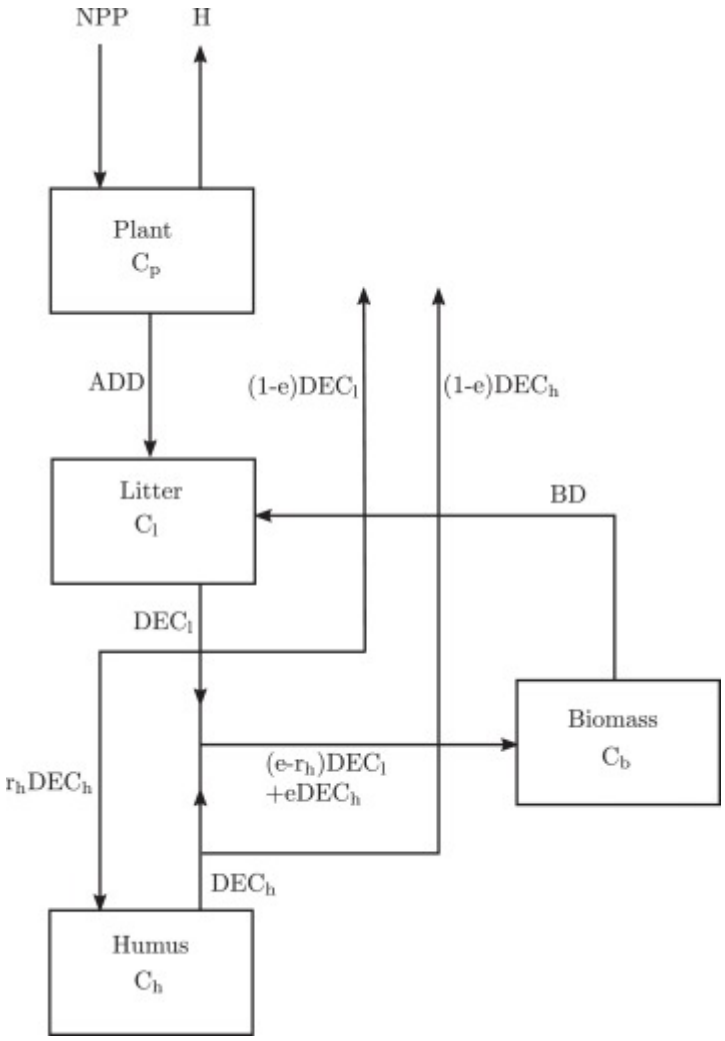

Fig. 1. Carbon balance model schematic. Fluxes are: net primary productivity (NPP), litter and humus decomposition (DECl and DECh), biomass harvest (H), litterfall (ADD), decomposer turnover (BD). Pools are: plant (p), fast-cycling litter (l), slow-cycling humus (h), and decomposers (b). The fraction of decomposed litter partitioned to humus is rh and the heterotrophic carbon use efficiency is e.

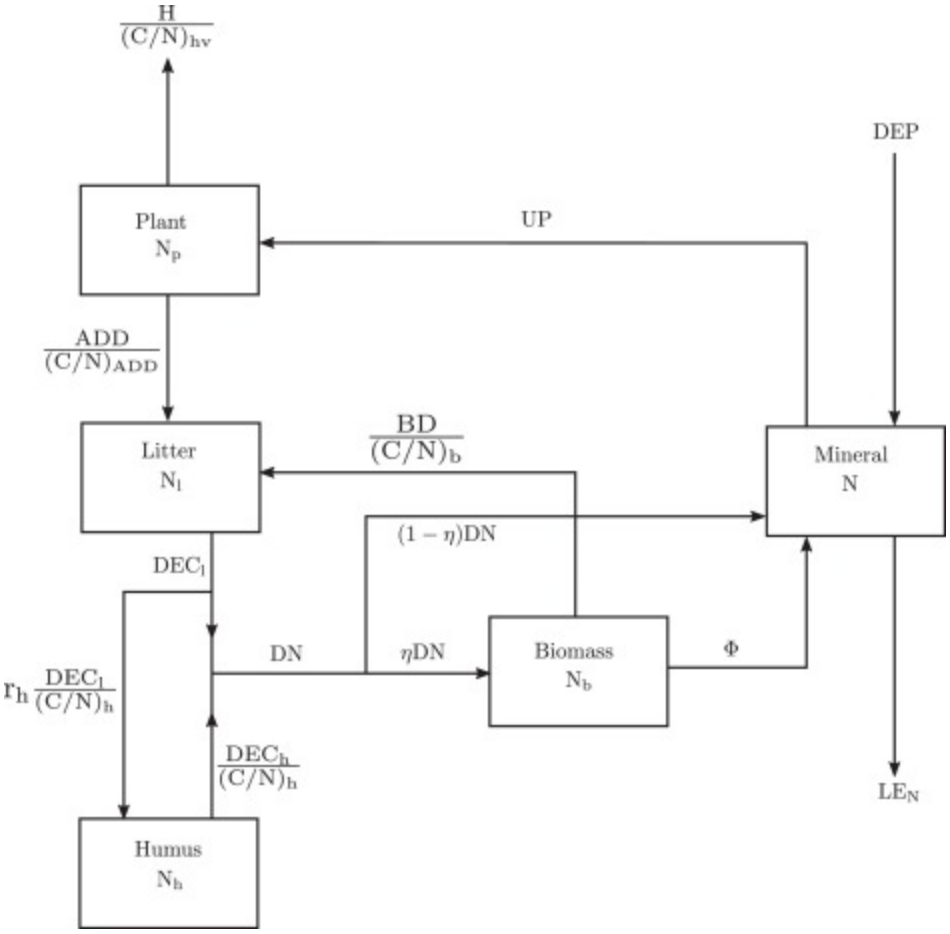

Fig. 2. Nitrogen balance model schematic. Fluxes are: deposition (DEP, which may include wet/dry mineral deposition and fertilization), leaching ($\mathrm{LE_N}$), harvest (H), litter and humus decomposition (DECl and DECh), litterfall (ADD), decomposer turnover (BD), nitrogen flux released during decomposition (DN), and the decomposer N demand (Φ). Pools are: plant (p), fast-cycling litter (l), slow-cycling humus (h), decomposers (b), and mineral N (no subscript). A fraction (η) of DN is directly assimilated into microbial biomass. The fraction of decomposed litter partitioned to humus is r_h and the C:N ratios are denoted as (C/N)x.

There is no shortage of studies that quantified the impact of biomass harvest on soil C and N storage and associated soil biogeochemical process rates. However, while biomass harvest inevitably intensifies ecosystem C and N losses, there is little consensus on the magnitude and direction of the aggregate effects on soil C storage, soil C and N fluxes, and primary production. In a meta-analysis of 73 studies, Johnson and Curtis (2001) found no change in soil C and N storage after harvest, although individual studies showed positive or negative changes. In contrast, a meta-analysis of 432 studies in temperate forests showed harvesting decreased forest floor C storage by 30% on average (Nave et al., 2010). Although many studies demonstrated soil C losses under harvest, full recovery of C storage is common after several decades (Covington, 1981, Guo and Gifford, 2002, Peng et al., 2002, Wei et al., 2003, Yanai et al., 2003, Nave et al., 2010). With regard to N fluxes, clearcut harvest was found to increase N availability, nitrification, and mineralization across more than 54 studies (Jerabkova et al., 2011). Similar to changes in C storage, these effects disappeared 10–15 years after harvest. In general,

soil biogeochemical impacts after harvest were attributed to harvest type (i.e., whole-tree, stem-only), species, fertilization, and the time of post-harvest sampling. In addition to the large amount of uncertainty in these results, the time-dependence of post-harvest ecosystem function underscores the importance of identifying the time-scales of transient disturbance responses in harvested ecosystems with models.

Many previous studies modeled the soil biogeochemical cycle response to management practices (e.g., Aber et al., 1982, Rolff and Agren, 1999, Thornley and Cannell, 2000, Peckham et al., 2013, Dangal et al., 2014) and a subset purposely analyzed the relation between harvest and the internal dynamics of soil C–N cycles (Dewar and McMurtrie, 1996a, Dewar and McMurtrie, 1996b, Corbeels et al., 2005, Tian et al., 2012, Wang et al., 2014). These modeling studies noted residue removal and increased soluble inorganic nitrogen leaching after harvest as primary sources of N loss in harvested ecosystems, which may reduce primary production over time. Because harvest residue constitutes the main source of organic N to decomposers and the pool of inorganic N available for leaching results from the balance of plant and decomposer N demand, it is anticipated such modeling results are sensitive to the underlying modeling structure. Recent advances in the modeling of C–N cycle dynamics emphasized the strength of nutrient competition between plants and decomposers and the coupling of decomposer population dynamics to the decomposition rate (Johnson, 1992, Schimel and Bennett, 2004, Manzoni and Porporato, 2007). Further understanding of these processes in harvested ecosystems may yield new insight regarding the management of soil C–N cycles to reduce N losses (Goulding et al., 2008).

To make progress on this topic, the impact of ecosystem management practices on soil C–N cycles is studied in a model ecosystem of intermediate complexity. Specifically, we consider the plant–soil C–N cycle feedbacks and the balance of N mineralization and immobilization during SOM decomposition in response to N fertilization and harvest intensity, defined as the quantity (i.e., mass), quality (i.e., C to N ratio (C:N)), and frequency of harvest. We present analytical, steady-state solutions to a simplified system harvested at a continuous and constant rate as well as numerical simulations of systems subject to repeated clear-cut harvest and re-growth. Continuous harvest is analogous to the selection method, in which a small fraction of the forest is harvested and replaced at short intervals (Smith et al., 1997). From these model results, harvested ecosystem function is discussed with respect to ecosystem services including biomass yield, standing biomass, and soil biogeochemical cycling.

2. Model of coupled plant–soil carbon–nitrogen dynamics

The model developed here combines the soil C–N cycling schemes proposed by Porporato et al. (2003) and Manzoni and Porporato (2007) coupled to a model for the plant C–N dynamics. This coupled plant–soil C–N model has nine pools as state variables: four carbon and five nitrogen pools.

The soil model describes three soil organic matter pools (litter, humus, and decomposer biomass), each with associated C and N, and one mineral N pool.

Several model assumptions are employed to parameterize C and N fluxes and to reduce model complexity. Decomposition follows a flexible scheme that merges the mineralization-immobilization turnover (MIT) and direct assimilation (DIR) hypotheses (Manzoni and Porporato, 2009). Further, three decomposition functions are tested to evaluate the consequences of coupling substrate and decomposer dynamics. The model assumes a constant C:N for the plant, humus, and decomposer pools and a variable litter C:N, which reduces the number of state variables from nine to six. The model is applied at the annual time-scale and inter-annual variations in climate are ignored. The model, with additional assumptions, is described below and depicted in Fig. 1, Fig. 2.

The C balance equations for plant $(\mathrm{C_p})$, litter $(\mathrm{C_l})$, humus $(\mathrm{C_h})$, and decomposer biomass $(\mathrm{C_b})$ are:

(1)

$$\frac{dC_p}{dt} = NPP - LF - H,$$

(2)

$$\frac{dC_l}{dt} = ADD + BD - DEC_l,$$

(3)

$$\frac{dC_h}{dt} = r_h DEC_l - DEC_h,$$

(4)

$$\frac{dC_b}{dt} = eDEC_h + (e - r_h)DEC_l - BD,$$

where the fluxes are net primary productivity (*NPP*), plant litterfall (*LF*), harvest (*H*), litter addition (*ADD*) (which includes both *LF* and harvest residue application), decomposer turnover (*BD*), and litter and humus decomposition $(\mathrm{DEC_x})$. A fraction r_h of the decomposed litter is partitioned to the humus pool and the carbon use efficiency, *e*, represents the fraction of the litter and humus decomposition flux assimilated into the decomposer biomass (i.e., $r = 1 - e$ is the respired fraction).

The N balance equations for the dynamic litter $(\mathrm{N_l})$ and mineral (*N*) nitrogen pools are:

(5)

$$\frac{dN_l}{dt} = \frac{ADD}{(C/N)_{add}} + \frac{BD}{(C/N)_b} - \frac{DEC_l}{(C/N)_l}$$

and

(6)

$$\frac{dN}{dt} = DEP - UP + (1-\eta)DN + \Phi - LE_N,$$

where the litter N fluxes are equal to the ratios of the associated C fluxes and C:N ratios, denoted as $(C/N)_x$ for pool *x*. The mineral N fluxes are aerial deposition (*DEP*), which includes fertilization, plant uptake (*UP*), direct mineralization from decomposition (*DN*), the net of decomposer mineralization and immobilization (Φ), and leaching losses ($\mathrm{LE_N}$). A fraction η, the microbial N-assimilation efficiency, of the N released in decomposition is directly assimilated by the decomposers. Because constant C:N is assumed for the plant, humus, and decomposer pools, their N balances are given directly by their C balance equations.

This six-pool model is of minimum complexity, but includes the essential nonlinearities, decomposer-litter feedbacks, and plant–soil feedbacks necessary to study these dynamics. Assumptions for the fluxes between pools are now described.

2.1. Plant carbon and nitrogen fluxes

Plant biomass, C_p, is simulated as the balance between net primary productivity and losses due to biomass turnover and harvest (Eq. (1)). *NPP* sensitivity to soil N availability is conceptualized as a switch between C- and N-limited productivity. When N uptake is not limiting, we assume *NPP* follows logistic growth that saturates with C_p. This productivity regime is termed “C-limited” because it accounts for several physical environmental factors, such as light, soil moisture, and temperature that may limit carbon uptake, but are not explicitly modeled. To account for limitation by N availability, we assume *NPP* is controlled by the potential rate of soil N uptake. Soil N uptake is modeled as $k_{up}N$ where k_{up} (yr^{-1}) is an uptake capacity that integrates the physical and microbial processes controlling N transport to the root surface and the kinetics of N uptake enzymes.

Because the plant organs are lumped into a single plant pool, some care is needed to define the plant carbon and nitrogen fluxes. Low C:N leaves turnover more quickly than high C:N stems and, therefore, plant N cycles more quickly than plant C. The litterfall C flux is modeled as a constant fraction, m_p (yr^{-1}), of C_p,

(7)
$$LF = m_p C_p$$

and we assume the rate of litterfall N flux is related to m_p by a factor f_N, $LF_N = f_N LF(C/N)_p^{-1}$. Note that this formulation implicitly accounts for retranslocated leaf N (Vergutz et al., 2012) in the parameter f_N.

With the above assumptions, the expression for *NPP* is,

(8)
$$NPP = \min\left[gC_p\left(1 - \frac{C_p}{K}\right), (k_{up}N - (f_N - 1)m_p N_p)(C/N)_p\right],$$

where g (yr^{-1}) is the biomass-specific density-independent growth rate and K $(\mathrm{g\ C\ m}^{-2})$ is the carrying capacity. Finally, note that for constant $(\mathrm{C/N})_\mathrm{p}$, plant N uptake is given by Eq. (8),

(9)
$$UP = (NPP + (f_N - 1)m_p C_p)(C/N)_p^{-1}$$

Eqs. (8), (9) reflect that the litterfall is enriched in N relative to the lumped plant pool and adjust the carbon and nitrogen inputs accordingly.

2.2. Biomass harvest fluxes

Our analysis utilizes two harvesting schemes: “continuous” and clear-cut “rotational” harvest. Continuous harvest is analogous to uneven-aged management in which a small fraction of the forest is harvested and replaced with younger trees on a nearly continuous basis, whereas rotational harvest represents a forest in which all trees are removed on a periodic basis (Smith et al., 1997). The harvest model can accommodate whole-tree and stem-only harvest practices by varying the relative masses of C and N removed from the system during harvest. Example system trajectories comparing each scheme are plotted in Fig. 4.

2.2.1. Continuous harvest

Under continuous harvest, a fraction of plant biomass is removed continuously in time. The characteristics of the harvest are defined in terms of the quantity and quality of biomass removed. Harvest quantity is defined as a constant fraction of standing biomass removed per unit time, f_{hv}. Secondly, we assume a residual fraction, a, of the harvested biomass is returned to the litter pool, such that,

(10)
$$H = (1 - a) f_{hv} C_p$$

And

(11)
$$ADD = LF + a f_{hv} C_p = (m_p + a f_{hv}) C_p.$$

Harvest quality is defined as the C:N of the harvested biomass, $(C/N)_{hv}$. $(C/N)_{hv}$ varies across tree species and harvest type, depending on whether leaves and other harvest residue is exported or maintained on site. Note that $(C/N)_{hv}$ in cropping systems, where fruit and leaves are harvested, is lower than that in forestry systems where wood is harvested. The N contained in litterfall and harvest residue is,

(12)
$$\frac{ADD}{(C/N)_{add}} = \frac{f_N m_p C_p}{(C/N)_p} + f_{hv} C_p \left(\frac{1}{(C/N)_p} - \frac{1-a}{(C/N)_{hv}} \right) \geq 0,$$

where the first term on the RHS is the litter N production from natural turnover processes and the second term accounts for differences between $(\mathrm{C/N})_{\mathrm{p}}$ and $(C/N)_{hv}$ that determine the quality of harvest residue returned to the litter pool. The inequality in Eq. (12) ensures the total N removed from the ecosystem does not exceed that available in the harvested biomass. The C:N of the aggregate plant residues can then be computed by noting that the plant litter C flux is $ADD = (m_p + a f_{hv}) C_p$,

(13)
$$\frac{1}{(C/N)_{add}} = \frac{f_N m_p}{(m_p + a f_{hv})(C/N)_p} + \frac{f_{hv}}{m_p + a f_{hv}} \left(\frac{1}{(C/N)_p} - \frac{1-a}{(C/N)_{hv}} \right)$$

According to Eq. (13), when the harvest is enriched in N relative to the residues (i.e., $(C/N)_{hv}(1 - a)^{-1} < (C/N)_p$, the litter N flux is decreased to account for the additional N export. Similarly, when the harvest is depleted in N relative to the residues (i.e., $(C/N)_{hv}(1 - a)^{-1} > (C/N)_p$, the litter N flux is increased to account for the additional N retention.

2.2.2. Clear-cut rotational harvest

In clear-cut rotational systems, all harvested trees are removed from the plot simultaneously within a relatively short period of time. The harvest function in this case is defined as a concentrated pulse at regular intervals,

(14)
$$H(t) = C_p \delta(t - \tau_r n),$$

where n = 0, 1, 2, … is the rotation number, τ_r is the rotation length, and $\delta(\cdot)$ is the Dirac delta function which turns on the instantaneous harvest at regular intervals of time. At the time of each harvest, the finite quantity $(1 - \mathrm{a})\mathrm{C_p}$ with $(C/N)_{hv}$ is removed from the system and a quantity of residual aC_p is added to the litter pool. From the harvest N balance, the C:N of this residual can be computed as,

(15)

$$(C/N)_{res} = a\left(\frac{1}{(C/N)_p} - \frac{1-a}{(C/N)_{hv}}\right)^{-1}.$$

Eq. (15) is only valid for $a > 0$, indicating a positive harvest residual flux to the litter pool.

2.3. Soil carbon and nitrogen fluxes

The remaining soil C and N fluxes include deposition and fertilization, decomposer turnover, decomposition, mineralization-immobilization, and leaching. We assume a constant deposition rate, *DEP*, and linear functions for decomposer turnover, $BD = m_b C_b$, and mineral N leaching, $LE = k_s N$. To explore the consequences of modeling nonlinearities in the soil C–N cycle, we consider three decomposition functions: linear,

(16)

$$DEC_x = \phi k_x C_x,$$

multiplicative,

(17)

$$DEC_x = \phi k_x C_x C_b,$$

and Michaelis–Menten,

(18)

$$DEC_x = \phi \frac{k_x C_x C_b}{K_x + C_x},$$

where the subscript x refers to the litter or humus pools, k_x is the decomposition rate, and K_x is the half-saturation constant.

The term ϕ in Eqs. (16), (17), (18) is the ratio of the maximum immobilization rate to the microbial immobilization demand (i.e., $\phi = -IMM_{max}/\Phi$ for $\Phi < 0$) and controls the switch between C- and N-limited decomposition regimes. Similar to plant productivity, the decomposer N demand relative to the supply from litter, humus, and mineral N determines the limiting factor for decomposition. To derive ϕ, two assumptions are made: (1) constant C:N for decomposer biomass, $(\mathrm{C/N})_\mathrm{b}$, which defines

the immobilization demand, and (2) a maximum immobilization rate equivalent to $k_I N C_b$ (Porporato et al., 2003). These assumptions lead to,

(19)
$$\phi = \frac{k_I N C_b}{DEC_h\left(\frac{e}{(C/N)_b}-\frac{\eta}{(C/N)_h}\right)+DEC_l\left(\frac{e-r_h}{(C/N)_b}+\frac{\eta r_h}{(C/N)_h}-\frac{\eta}{(C/N)_l}\right)},$$

where the denominator is equal to Φ. This quantity was previously derived for a two-pool SOM system with MIT-DIR scheme (Manzoni and Porporato, 2007; see also Manzoni and Porporato, 2009) and a three-pool SOM system with a strict DIR scheme (i.e., the microbial N-assimilation efficiency, $\eta = 1$) (Porporato et al., 2003). The present model is a combination of these two approaches, coupling a three-pool SOM system with the MIT-DIR scheme. Previous work has shown that a three-pool SOM model is a minimally complex model that captures a large proportion of SOM dynamics (Bolker et al., 1998) and that the flexible MIT-DIR scheme accounts for the spectrum of plant-decomposer competition for mineral N encountered in real soils, a primary source of nonlinearity in SOM systems (Manzoni and Porporato, 2007).

2.4. Model parameterization

Model parameters were chosen to represent the relatively well-characterized Loblolly Pine (*Pinus taeda*) plantations of the Southeastern United States. In particular, data were obtained from the Calhoun Long-Term Soil Ecosystem (LTSE) experiment (Richter et al., 2000, Mobley, 2011, Mobley et al., 2013, Mobley et al., 2015). We assume the soil observations correspond to the non-harvested steady-state and the plant observations correspond to recovery following a single harvest applied to the non-harvested steady-state. Following harvest, the plant carbon pool is initialized at 5 Mg C ha^{-1}. Beginning at age 40, the Calhoun LTSE experienced a period of decline in tree biomass, which has so far eluded explanation (Mobley, 2011). Therefore, we further assume that the peak tree biomass, which was obtained between age 26 and 31, corresponds to the non-harvested steady-state. Parameters and references for this system are summarized in Table 1 and the model performance is demonstrated in Fig. 3 and Table 2. Example trajectories of continuously harvested and clear-cut rotational systems are plotted in Fig. 4.

Table 1. Model parameters for Southeastern US Loblolly Pine plantation.

Parameter	Units	Value	Reference
Plant carrying capacity, ***K***	Mg C ha^{-1}	139	a
Plant growth rate, ***g***	yr^{-1}	0.25	a
Plant C turnover rate, $\boldsymbol{m_p}$	yr^{-1}	0.02	b

Parameter	Units	Value	Reference
Plant N turnover factor, f_N	–	1.87	[b]
Plant C:N, $(C/N)_p$	–	293	[b]
N uptake coefficient, k_{up}	yr^{-1}	0.5	–
N deposition rate, DEP	kg N ha^{-1} yr^{-1}	10	Richter and Markewitz (1995)
N leakage coefficient, k_s	yr^{-1}	0.05	–
Maximum immobilization rate, k_I	d^{-1} g C^{-1} m^{-2}	2	D'Odorico et al. (2003)
Decomposer N efficiency, η	–	0.4	Manzoni and Porporato (2007)
Decomposer turnover, m_b	yr^{-1}	0.14	[c]
Decomposer C use efficiency, e	–	0.25	Brady and Weil (2004)
Decomposer C:N, $(C/N)_b$	–	10	Manzoni and Porporato (2007)
Humus C:N, $(C/N)_h$	–	22	Mobley et al. (2015)
Litter decomposition rate, k_l	yr^{-1}	2.2e−4	[c]
Humus decomposition rate, k_h	yr^{-1}	4.8e−5	[c]
Fraction of decomposed litter partitioned to humus, r_h	–	0.2	Brady and Weil (2004)

[a] *NPP* parameters were estimated by fitting Eq. (1) to measurements of total biomass carbon measured at the Calhoun Experimental Forest (Mobley, 2011).
[b] Plant C and N turnover rates and C:N were estimated from measurements (Jorgensen et al., 1980, Mobley, 2011); and assuming a leaf N retranslocation fraction of 0.6 (Vergutz et al., 2012).
[c] Decomposition and decomposer turnover rates were estimated assuming observed carbon pools are equivalent to the steady-state modeled values.

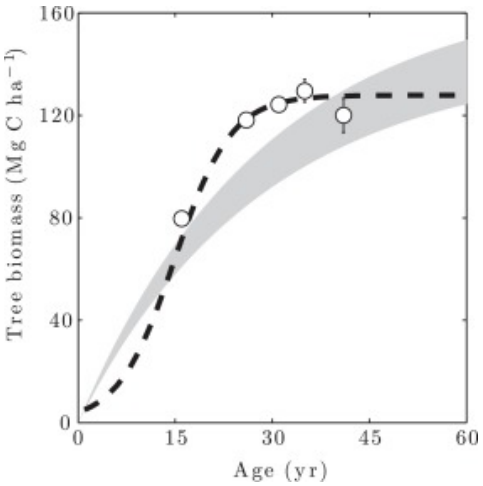

Fig. 3. Comparison of observed and modeled tree biomass carbon trajectories following disturbance. "FIA model" and the gray region refer to a model fit to the regional Forest Inventory and Analysis dataset by Williams

et al. (2012). “Calhoun LTSE” and the open circles refer to observations from the Calhoun Long-Term Soil-Ecosystem Study in South Carolina (Mobley, 2011). Parameters for the present model (dashed line) are listed in Table 1.

Table 2. Comparison between non-harvested model steady-state and plant and soil carbon and nitrogen pools and fluxes previously observed and estimated for the Calhoun LTSE.

Pool/flux	Units	Modeled	Observed	Reference
Plant carbon, C_p	g C m^{-2}	12,790	12,960 ± 1250	Mobley (2011)
Litter carbon, C_l	g C m^{-2}	4531	4531 ± 785	Mobley (2011)
Humus carbon, C_h	g C m^{-2}	3096	3096 ± 329	Mobley (2011)
Decomposer carbon, C_b	g C m^{-2}	300	85 ± 9[a]	Xu et al. (2013)
Total ecosystem N, $\sum N$	g N m^{-2}	306	297 ± 34	Richter et al. (2000)
SOM C:N ratio, –	g C g N^{-1}	32.7	29	Mobley et al. (2015)
Net mineralization, MIN_{net}	g N m^{-2} yr^{-1}	1.6	1.21	Richter et al. (2000)
N leaching, L_N	g N m^{-2} yr^{-1}	1	<0.1	Richter et al. (2000)

[a]Xu et al. (2013) estimate microbial biomass accounts for approximately 1.8% of soil organic carbon in tropical/subtropical forest.

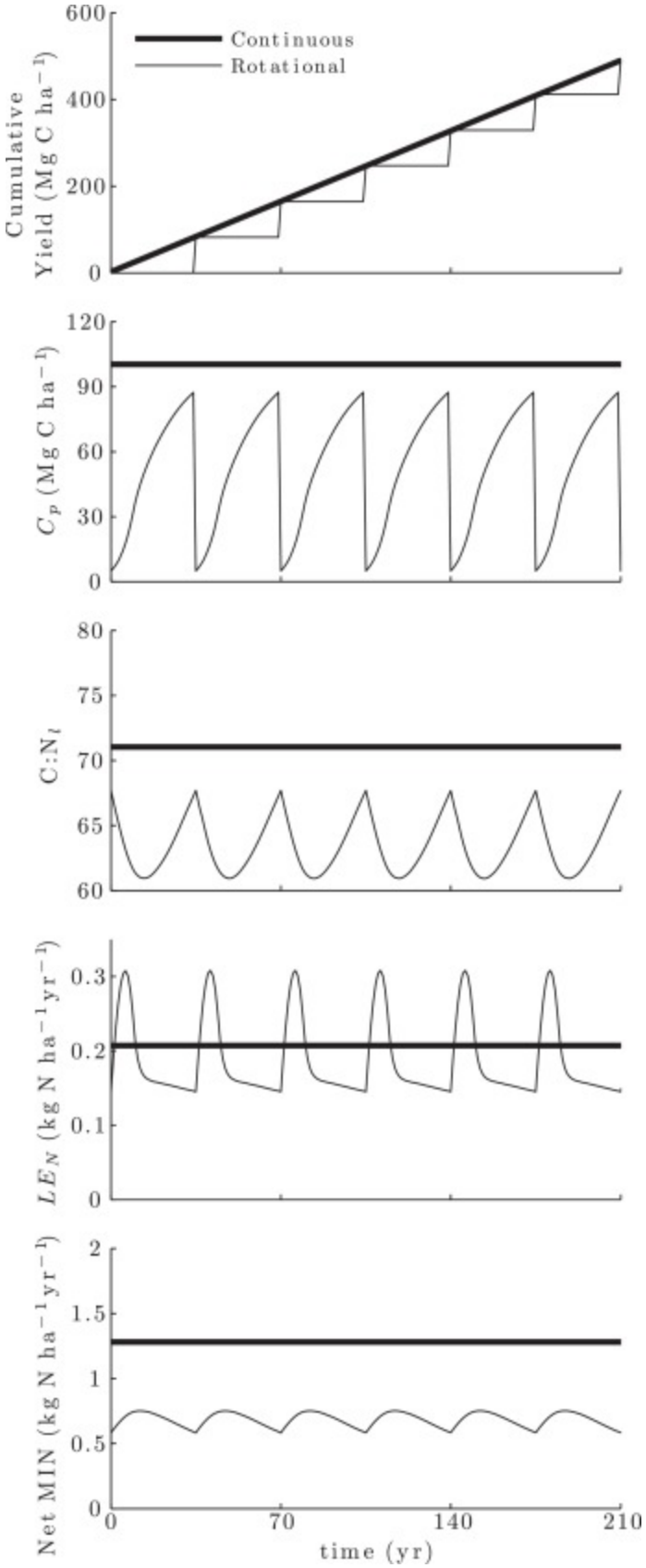

Fig. 4. Example trajectories of continuously-harvested (bold lines) and clear-cut rotational (thin lines) ecosystems. f_{hv}=0.0232 for continuous harvest, τ_r = 35 years for rotational harvest, $(C/N)_{hv} = (C/N)_p$, $a = 0$, and all other parameters are listed in Table 1.

3. Continuously-harvested ecosystems

In this section, dynamics of the continuous harvest system with the harvest function described in Section 2.2.1 are discussed, including the steady-state solutions and transient behavior.

3.1. Steady-state solutions

For $f_{hv} \geq 0$ constant, the steady-state C and N pool sizes and fluxes can be determined analytically from the system equations. The steady states are calculated for each decomposition function defined in Eqs. (15), (16), (17) and denoted by an asterisk below. The solutions differ in the number of functional steady states, i.e., those that are stable and have realistic, finite values with positive C_p, and in their dependence on the harvest strategy and fertilization rate.

The functional steady states are summarized in Table 3. The linear decomposition model contains a second unstable steady state, with all state variables equal to zero except $N* \ = DEP/k_s$. The multiplicative and Michaelis–Menten models each contain two degenerate solutions where $C_p^* = C_b^* = 0$, $N* \ = DEP/k_s$, and at least one other state is not uniquely defined by the system equations. At steady state, the system is unable to maintain positive C_p^* when $f_{hv} > g - m_p$, which defines the maximum allowable harvest intensity.

Table 3
Steady-state solutions for the continuously-harvested system using linear, multiplicative, and Michaelis–Menten decomposition functions. Other state variables not listed here (i.e., N_p, N_h, and N_b) are given by the C:N ratios of the respective pools, assumed constant. These are stable, functional steady-states with positive plant biomass. Other solutions are outlined in the text.

DEC	Linear $k_l C_l$	Multiplicative $k_l C_l C_b$	Michaelis–Menten $\frac{k_l C_l C_b}{K_l + C_l}$
C_p^*	$\min\left[K \ 1-\frac{m_p+f_{hv}}{g}\right), \frac{(C/N)_{hv}(C/N)_p DEP k_{up}}{(1-a)(C/N)_p f_{hv} k_{up}+(C/N)_{hv} k_s (f_{hv}+f_N m_p)}$	$\min\left[K \ 1-\frac{m_p+f_{hv}}{g}\right), \frac{(C/N)_{hv}(C/N)_p DEP k_{up}}{(1-a)(C/N)_p f_{hv} k_{up}+(C/N)_{hv} k_s (f_{hv}+f_N m_p)}$	$\min\left[K \ 1-\frac{m_p+f_{hv}}{g}\right), \frac{(C/N)_{hv}(C/N)_p DEP k_{up}}{(1-a)(C/N)_p f_{hv} k_{up}+(C/N)_{hv} k_s (f_{hv}+f_N m_p)}$
N^*	$k_s^{-1}\left(DEP-\frac{(1-a)f_{hv}C_p^*}{(C/N)_{hv}}\right)$	$k_s^{-1}\left(DEP-\frac{(1-a)f_{hv}C_p^*}{(C/N)_{hv}}\right)$	$k_s^{-1}\left(DEP-\frac{(1-a)f_{hv}C_p^*}{(C/N)_{hv}}\right)$
C_b^*	$\frac{(m_p+af_{hv})[e-(1-e)r_h]}{m_b(1-e)(1+r_h)}C_p^*$	$\frac{(m_p+af_{hv})[e-(1-e)r_h]}{m_b(1-e)(1+r_h)}C_p^*$	$\frac{(m_p+af_{hv})[e-(1-e)r_h]}{m_b(1-e)(1+r_h)}C_p^*$
CN_l^*	$\frac{m_p(1-e)(1+r_h)}{m_p+af_{hv}} \ \frac{f_N m_p+f_{hv}}{(C/N)_p}-\frac{(1-a)f_{hv}}{CN_{hv}}\Big)+\frac{e-(1-e)r_h}{(C/N)_b} \ ^{-1}$	$\frac{(1-e)(1+r_h)}{m_p+af_{hv}} \ \frac{f_N m_p+f_{hv}}{(C/N)_p}-\frac{(1-a)f_{hv}}{(C/N)_{hv}}\Big)+\frac{e-(1-e)r_h}{(C/N)_b} \ ^{-1}$	$\frac{(1-e)(1+r_h)}{m_p+af_{hv}} \ \frac{f_N m_p+f_{hv}}{(C/N)_p}-\frac{(1-a)f_{hv}}{(C/N)_{hv}}\Big)+\frac{e-(1-e)r_h}{(C/N)_b} \ ^{-1}$
C_l^*	$\frac{m_p+af_{hv}}{k_l(1-e)(1+r_h)}C_p^*$	$\frac{m_b}{k_l[e-(1-e)r_h]}$	$\frac{K_l m_b}{k_l[e-(1-e)r_h]-m_b}$
C_h^*	$\frac{r_h k_l}{k_h}C_l^*$	$\frac{r_h k_l}{k_h}C_l^*$	$\frac{K_h m_b r_h}{k_h(e-rr_h)-m_b r_h}$

The steady-state solutions are sensitive to the decomposition model structure. For the multiplicative and Michaelis–Menten decomposition models, soil C storage at steady state, $C_l^* + C_h^*$, is independent of the harvest strategy (f_{hv} and $(C/N)_{hv}$); whereas the linear decomposition model is the only formulation that results in a long-term impact of biomass harvest on soil C storage. On the other hand, steady-state soil N storage and plant and decomposer biomass are affected by biomass harvest in all three models. With respect to the N fertilization rate, represented by *DEP*, the linear model predicts increased soil C storage with *DEP*, whereas the multiplicative and Michaelis–Menten models predict no change. The sensitivity to model structure arises from decomposer biomass limitation of decomposition, which is present in the multiplicative and Michaelis–Menten models and not in the linear model.

Soil N cycling at steady state is characterized by the internal N fluxes, which are computed from the system equations and states listed in Table 3 (results from here forward are based on the multiplicative decomposition model for illustrative purposes). The possible steady-state soil N cycling regimes are plotted in Fig. 5 as a function of f_{hv} and $(C/N)_{hv}$. At steady state, the N cycle must operate under net mineralization conditions. These conditions are either pure mineralization with no immobilization (Regime A) or net mineralization, with positive net mineralization and positive immobilization (Regime B) (Manzoni and Porporato, 2007). In Regime A, when immobilization is zero,

(20)

$$MIN^*_{gross} = MIN^*_{net} = \left(\frac{f_N m_p + f_{hv}}{\left(\frac{C}{N}\right)_p} - \frac{(1-a) f_{hv}}{\left(\frac{C}{N}\right)_{hv}} \right) C^*_p,$$

which is equivalent to the nitrogen flux in the plant litter production (i.e., $ADD^*/(C/N)^*_{add}$). In Regime B, when immobilization is positive,

(21)

$$MIN^*_{gross} = ADD^*(1-\eta) \left[\frac{e-(1-e)r_h}{(1-e)(1+r_h)} \frac{1}{\left(\frac{C}{N}\right)_b} + \frac{1}{\left(\frac{C}{N}\right)^*_{add}} \right],$$

and

(22)

$$IMM^*_{gross} = ADD^*(1-\eta) \left[\frac{e-(1-e)r_h}{(1-e)(1+r_h)} \frac{1}{\left(\frac{C}{N}\right)_b} - \frac{\eta}{1-\eta} \frac{1}{\left(\frac{C}{N}\right)^*_{add}} \right].$$

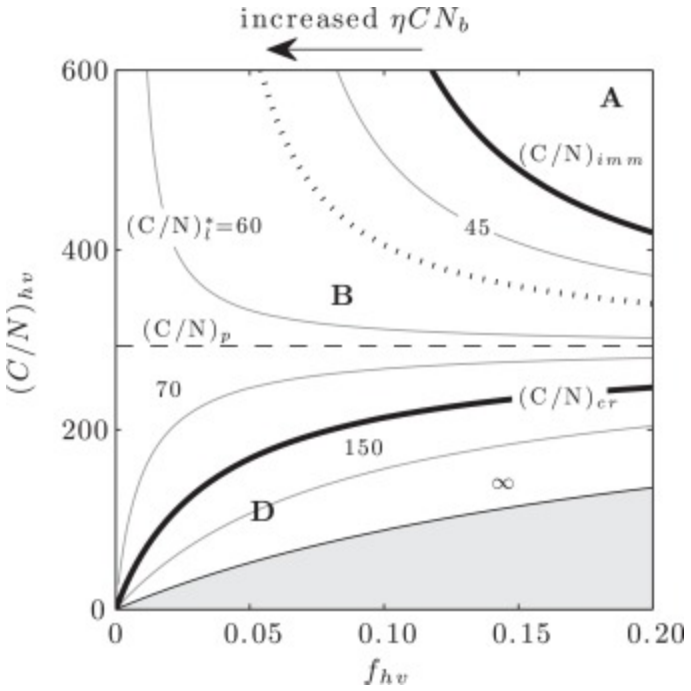

Fig. 5. Steady-state mineralization-immobilization regimes as a function of f_{hv} and $(C/N)_{hv}$ for continuous harvest with multiplicative decomposition model. The gray contours represent $(C/N)_l^*$ and the dashed line indicates $(\mathrm{C/N})_\mathrm{p}$. Parameters other than f_{hv} and $(C/N)_{hv}$ are listed in Table 1, except $a = 0$ and for the dotted line with $\eta = 0.5$.

In Eqs. (20), (21), (22), the influence of the harvest strategy on internal soil N cycling is found in f_{hv}, $(C/N)_{hv}$, a, and their influence on C_p^*, ADD^*, and $(C/N)_{add}^*$. The terms in the brackets of Eqs. (21), (22) indicate that, when immobilization is active, rates of mineralization and immobilization depend on a balance between the C:N of litter supply and demand as encoded in $(\mathrm{C/N})_{\mathrm{add}}$ and $(\mathrm{C/N})_\mathrm{b}$, respectively.

The expressions for net and gross mineralization and immobilization fluxes define the boundaries between steady-state N cycling regimes in the harvest strategy space (Fig. 5). The regime boundaries correspond to the steady-state litter C:N, as the harvest strategy directly determines the relative amounts of C and N returned to the soil as litter. The litter C:N at incipient immobilization (i.e., A/B boundary) is obtained by imposing $IMM_{gross}^* = 0$,

(23)

$$(C/N)_{imm} = \eta \frac{(C/N)_b}{e - (1-e)r_h}.$$

Similarly, the litter C:N where net mineralization switches to net immobilization is obtained by imposing $IMM_{gross}^* = MIN_{gross}^*$. Eqs. (21), (22) show that gross immobilization and mineralization are equal when $1/(C/N)_{add}^* = 0$. Therefore, using Eq. (13) and the solution for $(C/N)_l^*$ from Table 3, the boundary between net mineralization and net immobilization is,

(24)

$$\left(\frac{C}{N}\right)_{cr} = \frac{\left(\frac{C}{N}\right)_b}{e-(1-e)r_h}.$$

Eqs. (21), (24) demonstrate that the condition of net immobilization is controlled by a link between plant litter production and decomposer stoichiometry. The critical litter C:N, $(\mathrm{C/N})_{\mathrm{cr}}$, is only a function of the decomposer metabolic parameters and coincides with the point where plant litter N production ceases. That is, the ability of decomposers to maintain net mineralization depends on positive resupply of litter N from plant residues. Because the litter N flux must be positive, steady states with litter C:N above $(\mathrm{C/N})_{\mathrm{cr}}$ are unrealistic as they are unable to meet the imposed N export demand. Note, however, that transient systems may spend time under net immobilization conditions, as discussed below.

The regime occupied by the non-harvested system (i.e., $f_{hv} = 0$) is controlled by the microbial N-utilization efficiency, η. When microbes are inefficient at assimilating mineralized N (i.e., low η), immobilization from the mineral N pool is required to meet the microbial N demand and the system is in Regime B. On the other hand, efficient microbial N assimilation (i.e., high η) decreases immobilization requirements and the system is in Regime A. The point at which the non-harvested system shifts between Regime A and B is

(25)

$$\eta_{imm} = \left[1 + \frac{(1-e)(1+r_h)}{e-(1-e)r_h}\frac{f_N\left(\frac{C}{N}\right)_b}{\left(\frac{C}{N}\right)_p}\right]^{-1},$$

which again is independent of the harvest strategy, but depends on the relative stoichiometry of the plant and decomposer populations.

3.2. Steady-state biomass yield

The steady-state harvested biomass yield is computed as

(26)

$$Y = (1-a)f_{hv}C_p^* = \min[Y_C(f_{hv}), Y_N(f_{hv}, (C/N)_{hv})],$$

where Y_C and Y_N correspond to the C-limited and N-limited C_p^*, respectively (Table 3). The yield *Y* exhibits two regimes (Fig. 6): the first where $Y_N < Y_C$ for some range of f_{hv} and N-limited plant growth is possible; and the second where $Y_N < Y_C$ for all f_{hv} and C-limited plant growth prevails under all harvest intensities. When there is a surplus of N relative to C, the steady-state plant biomass and biomass yield are independent of the N cycle dynamics and only depend on the plant growth parameters and the harvest rate, f_{hv} Alternatively, when soil N availability limits productivity, biomass yield depends on many aspects of the soil N cycle – deposition rate, plant demand and uptake efficiency, leaching rate, and harvest quantity and quality. When N-limitation is present in the system, there exists a wide range of f_{hv} values that achieve similar biomass yield. For the parameters given in Table 1, sustainable harvest rates are within the range $0 < f_{hv} < 0.2$, a range consistent with estimates of logging probability calculated for northeastern US forests (Canham et al., 2013).

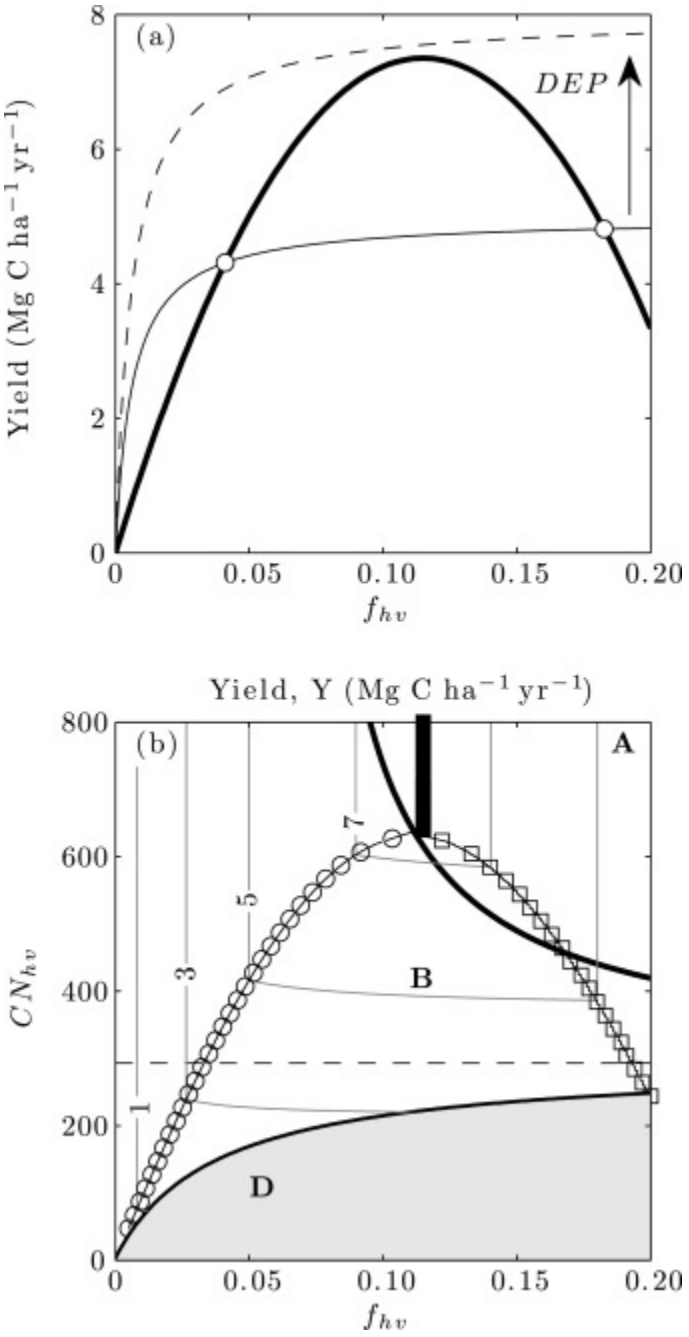

Fig. 6. Maximum sustainable yield (MSY) solutions for the continuously-harvested system. In (a), the open symbols mark the MSY solutions for co-limited conditions. The bold line is the carbon-limited MSY and the nitrogen-limited MSY is drawn for low (solid line) and high (dashed line) *DEP*. In (b), the symbols correspond to co-limited MSY (open squares), carbon-limited MSY (filled squares), and sub-optimal low-effort co-limited MSY (open circles). The contours represent yield and the regime boundaries are the same as in Fig. 5. Parameters other than f_{hv} and $(C/N)_{hv}$ are listed in Table 1, except $a = 0$ and in (a), $(C/N)_{hv} = (C/N)_p$ and the high and low *DEP* values are 32 and 20 kg N $ha^{-1}\ yr^{-1}$.

In harvested ecosystems with logistic-type growth patterns, there exists a maximum sustainable yield (MSY) that maintains the population density at a level that maximizes the growth rate. The MSY harvest rate balances the need for standing biomass to harvest with the density-dependent reduction

in growth rate at high densities. In our model, the MSY is calculated differently for the two yield regimes. Under C-limited conditions, the MSY is obtained from the condition $\partial Y_C/\partial f_{hv} = 0$,

(27)

$$Y_C^{MSY} = (1-a)\frac{gK}{4}\left(1-\frac{m_p}{g}\right)^2,$$

which is analogous to the classical result for logistic growth under continuous harvest (Murray, 2002). Under N-limited conditions, the MSY is the larger of the two solutions to $Y_C = Y_N$, which is quadratic in f_{hv}. N-limited conditions typically prevail at low $(C/N)_{hv}$, which indicates more intense harvest N export (Fig. 6b). In addition to $(C/N)_{hv}$, these MSY solutions are also controlled by the input and output of mineral N (i.e., *DEP* and k_s). The system response to *DEP* is shown in Fig. 6a.

The two N-limited solutions that satisfy $Y_C = Y_N$ correspond to a low-effort and high-effort harvest intensity, f_{hv}. The C_p^* solution in Table 3 shows that the yield difference between these two solutions depends on k_s, or the openness of the soil N cycle. However, this difference tends to be small, even for large k_s, and decays to zero as k_s goes to zero. Therefore, the low-effort solution could be considered a sub-optimal MSY that can be obtained at a substantial savings in effort.

Also in the N-limited growth regime, yield can be stimulated by N fertilization, which in our model is represented by *DEP*. As *DEP* increases, the range of f_{hv} under which the system is limited by soil N becomes narrower. Eventually, the system switches to a regime that is C-limited at all values of f_{hv}, where additional N inputs do not further increase yield and a single MSY associated with the C-limited yield curve emerges (i.e., Eq. (27)). The critical fertilization rate at which this switching occurs is obtained by equating the C-limited and N-limited expressions for biomass yield at the MSY harvest rate,

(28)

$$DEP_{crit} = \frac{K(g-m_p)}{4g\left(\frac{C}{N}\right)_{hv}\left(\frac{C}{N}\right)_p k_{up}}\left[(1-a)\left(\frac{C}{N}\right)_p k_{up}(g-m_p) + \left(\frac{C}{N}\right)_{hv} k_s\left(g-(1+2f_N)m_p\right)\right].$$

When $DEP = DEP_{crit}$, the true MSY of the system is accessible.

3.3. Transient system behavior

The continuously-harvested system exhibits a range of dynamical behavior in the vicinity of the steady-state (Fig. 7). In general, C-limited systems are characterized by a stable focus with one pair of complex

conjugates, indicating trajectories that spiral on a plane. N-limited systems are characterized by a stable focus with two pairs of complex conjugates, indicating trajectories that spiral on two orthogonal planes. This more complex behavior in N-limited systems suggests that plant–soil feedback is stronger when N limitation is present. The existence of stable spirals under a continuous harvest regime suggests the ecosystem disturbance response may be non-monotonic. That is, the direction of the soil biogeochemical response to harvest, which depends on the harvest strategy, may vary substantially as time passes after the disturbance. Such non-monotonic, oscillatory dynamics between SOM and decomposers were previously identified in controlled pot experiments (Zelenev et al., 2005). Some aspects of these disturbance-response trajectories are discussed in the context of N limitation under clear-cut harvest in Section 4.

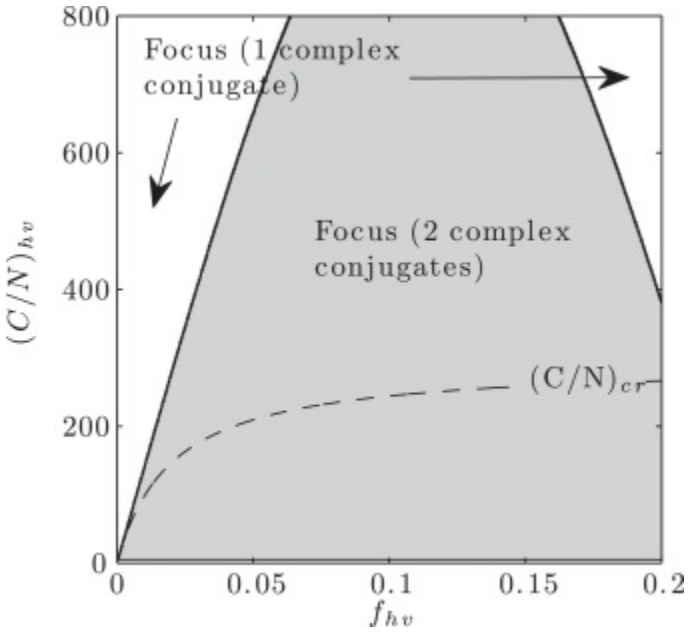

Fig. 7. Stability classification for the continuously-harvested steady-states as a function of f_{hv} and CN_{hv}. a = 0 and parameters other than f_{hv} and $(\mathrm{C/N})_{\mathrm{hv}}$ are listed in Table 1.

Under transient conditions, the soil N cycle may exhibit net immobilization or N-limited net mineralization. The transition between net mineralization and net immobilization is governed by $(\mathrm{C/N})_{\mathrm{cr}}$, defined in Eq. (24), whereas the transition between C-limited and N-limited microbial growth is governed by the maximum immobilization rate, $IMM_{\max} = k_I N C_b$. A condition for this latter transition can be derived by setting $\phi = 1$, which results in a complex expression relating the soil organic matter and mineral nitrogen pools. This threshold separates the N-limited microbial growth regimes (C and E) from their C-limited counterparts (B and D) (Manzoni and Porporato, 2007).

4. Clear-cut rotational ecosystems

In this section, dynamics of clear-cut, rotational harvest systems with the harvest function described in Section 2.2.2 are analyzed. The clear-cut system is a special case of the continuously-harvested system

that has the steady state for $f_{hv} = 0$ but is maintained away from this steady state by periodic harvest. The average system behavior during the steady-state rotation is investigated below with respect to the N fertilization rate, *DEP*, rotation length, τ_r, and decomposer respiration rate, r.

4.1. Plant–soil carbon–nitrogen cycling under clear-cut harvest

When the harvest is repeated indefinitely at a constant interval τ_r, clear-cut systems operate in a limit cycle at steady-state (Fig. 8). While the steady-state continuously-harvested systems always function in the net mineralization regimes (i.e., A and B), clear-cut systems at steady-state exhibit net mineralization on average but may spend time in the net immobilization regime (i.e., D) (Fig. 9). The switching between net mineralization and net immobilization regimes is controlled by the decomposer N demand, driven by the decomposition fluxes and C:N ratios of the various soil pools. Boundaries between the transient C–N cycling regimes can be described in terms of the SOM quality and the decomposition rate, accounting for both litter and humus pools. The A/B regime boundary, or point of incipient immobilization, can be written as,

(29)

$$\left(\overline{C/N}\right)_{imm} = \eta \frac{(C/N)_b}{e},$$

where the over-bar denotes the carbon flux-weighted harmonic mean of the C:N ratios associated with the fluxes from the litter and humus pools to the decomposer pool,

(30)

$$\left(\overline{C/N}\right) = \frac{eDEC_h + (e - r_h)DEC_l}{\frac{e}{(C/N)_h}DEC_h + \left(\frac{1}{(C/N)_l} - \frac{r_h}{(C/N)_h}\right)DEC_l}.$$

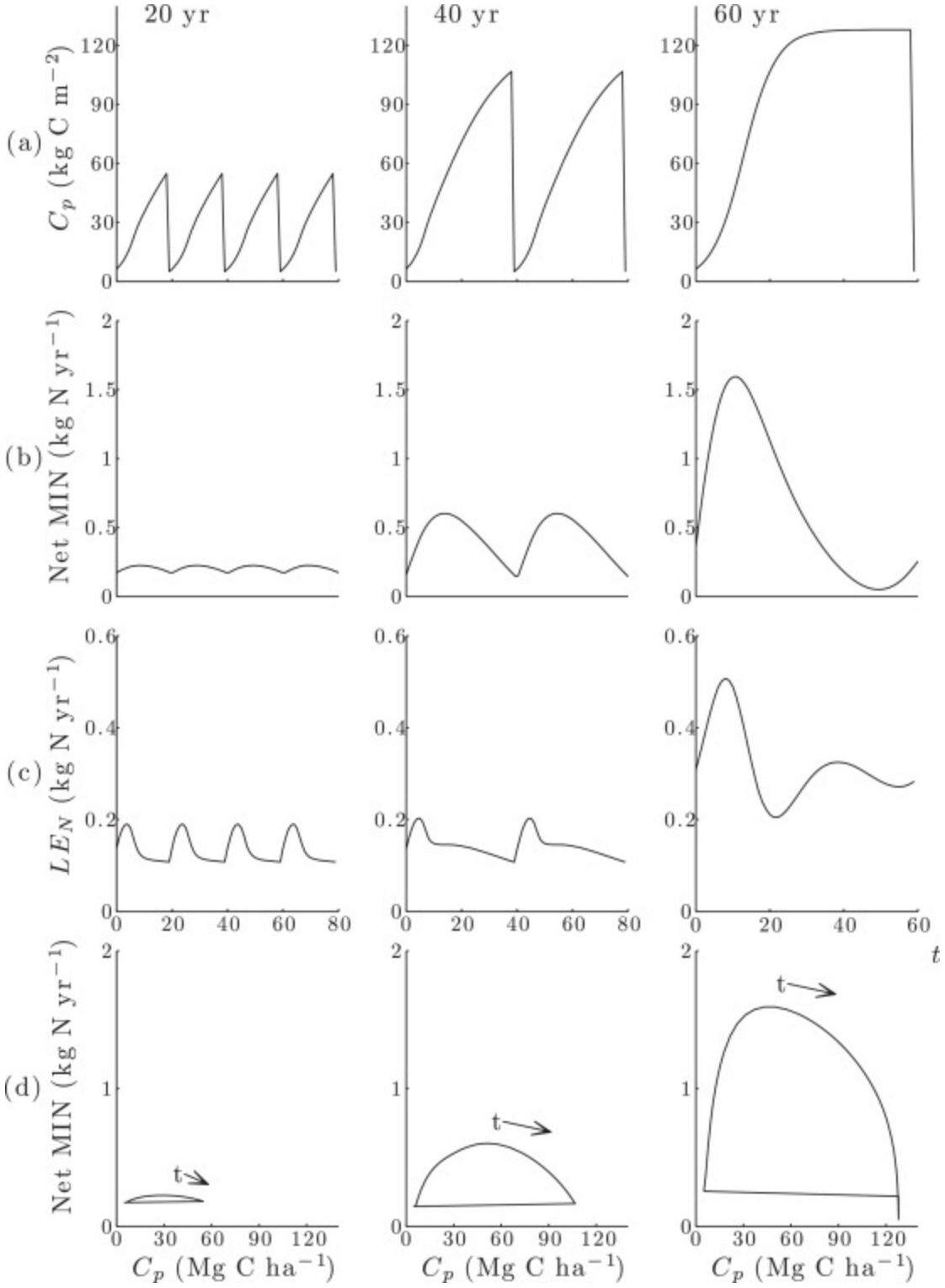

Fig. 8. Transient ecosystem dynamics under clear-cut rotational harvest for several rotation lengths: (a) plant biomass, (b) net mineralization, (c) N leaching, and (d) limit cycles in the net mineralization – plant biomass phase space. The rotation length τ_r is noted at the top of each column, $(C/N)_{hv} = (C/N)_p$, $a = 0$, and other parameters are listed in Table 1. The arrows in the bottom row show the direction of time.

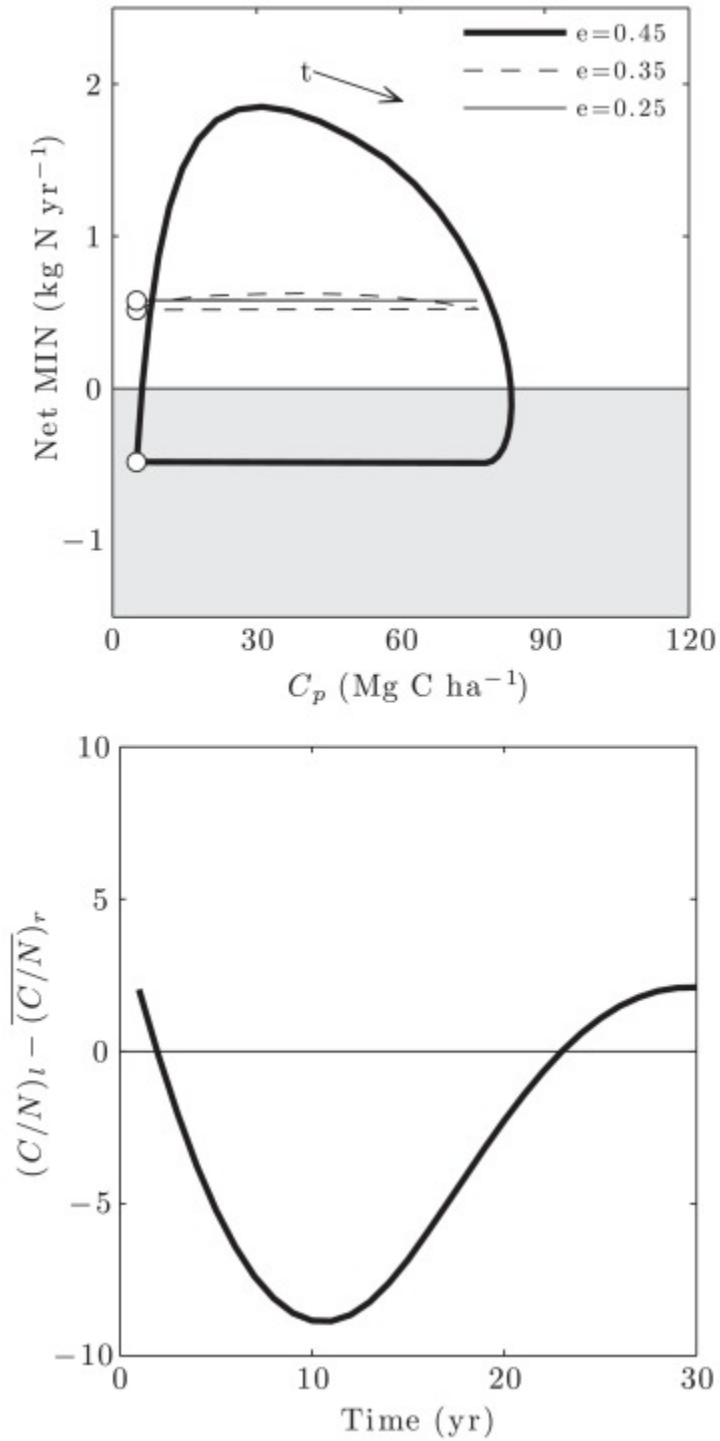

Fig. 9. Sensitivity of the clear-cut rotational plant–soil dynamics to the heterotrophic carbon use efficiency, e. $\tau_r = 30$ years, $(C/N)_{hv} = (C/N)_p$, $a = 0$, and other parameters are listed in Table 1. In (a), the open circles mark $t = 0$ and the arrow shows the direction of time. In (b), the difference between $(C/N)_l$ and the time-varying point of incipient net immobilization, $\overline{(C/N)}_{cr}$, defined in Eqs. (30), (31), is plotted for $e = 0.45$.

Similarly, the point where net mineralization equals zero marks the boundary between net mineralization and net immobilization,

(31)

$$\left(\overline{C/N}\right)_{cr} = \frac{(C/N)_b}{e}.$$

To study the role of decomposer N limitation on soil biogeochemical response to harvest, the transient ecosystem dynamics are plotted in Fig. 9 for several values of the decomposer respiration rate r, which alters $(\mathrm{C/N})_\mathrm{l}$, the flux of carbon assimilated by decomposers, and the decomposer mineral N demand. As r decreases and $(\mathrm{C/N})_\mathrm{l}$ increases, the system shifts from persistent net mineralization to a regime with alternating periods of net mineralization and net immobilization. In these systems, net immobilization is concentrated at the start and end of the rotation, whereas net mineralization occurs during the middle of the rotation (Fig. 9). Although net immobilization may occur for short periods, rotational systems always have positive net mineralization on average, consistent with the continuously-harvested system.

4.2. Biomass yield and ecosystem nitrogen-use efficiency under clear-cut harvest

In continuously-harvested systems, f_{hv} and $(C/N)_{hv}$ modify the steady-state yield; while in clear-cut systems, τ_r and $(C/N)_{hv}$ modify the transient regime repeatedly traversed in a steady limit cycle. The time-averaged fluxes during this cycle are now used to describe the function of the clear-cut system. Similar to previous studies, the model predicts an optimal rotation length that simultaneously maximizes yield and nitrogen-use efficiency (*NUE*) (Fig. 10, Fig. 11). Here, ecosystem-scale *NUE* is defined as the fraction of total nitrogen losses partitioned to harvest,

(32)

$$NUE = 1 - \frac{\overline{LE}_n}{DEP},$$

where $\overline{LE}_n$ is the time-averaged N leaching losses. Note, for this definition the maximum *NUE* is equivalent to minimum N leaching losses, however N may leave the system by other processes not modeled explicitly here, such as denitrification and N gas emission (e.g., Shcherbak et al., 2014) or leaching of dissolved organic N (Perakis and Hedin, 2002), but implicitly included in the inorganic N leaching term.

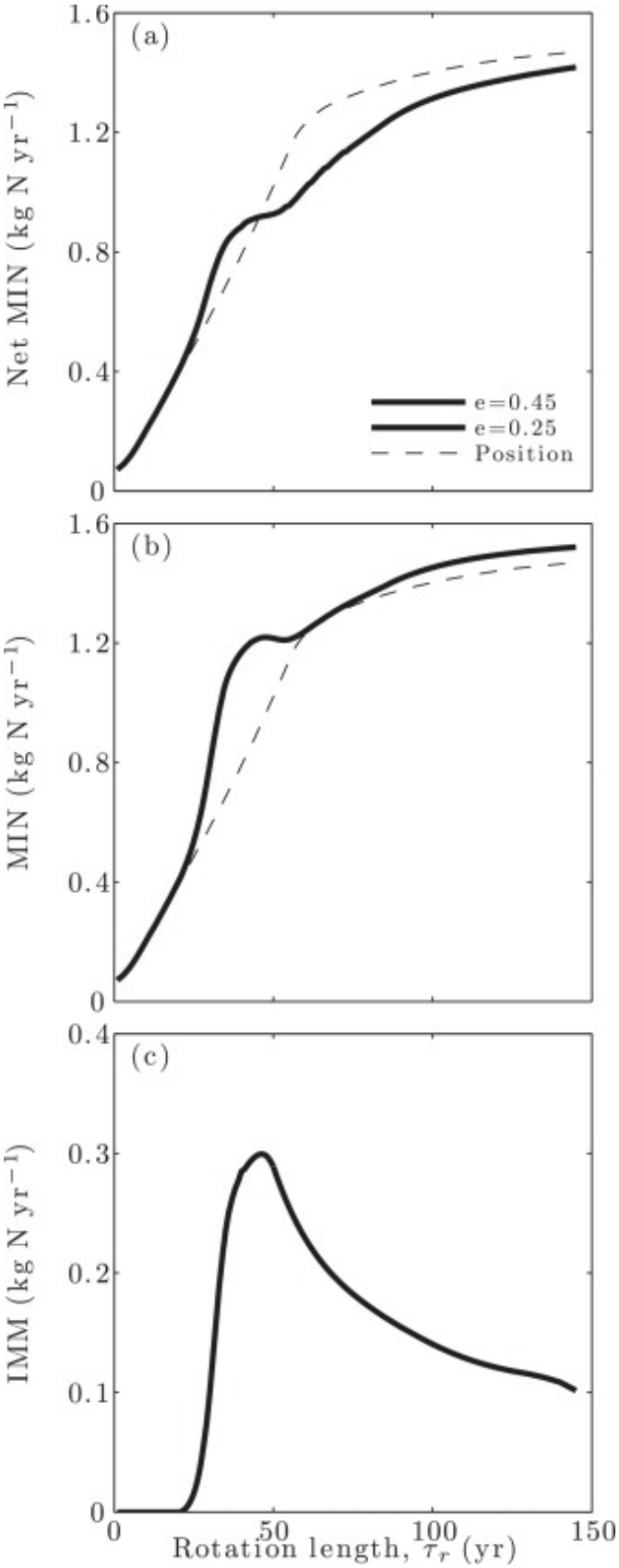

Fig. 10. Average soil N mineralization and immobilization fluxes under rotational harvest as a function of rotation length (τ_r) and heterotrophic carbon use efficiency (e): (a) net mineralization; (b) gross mineralization; and (c) gross immobilization. $(C/N)_{hv} = (C/N)_p$, $a = 0$, and other parameters are listed in Table 1.

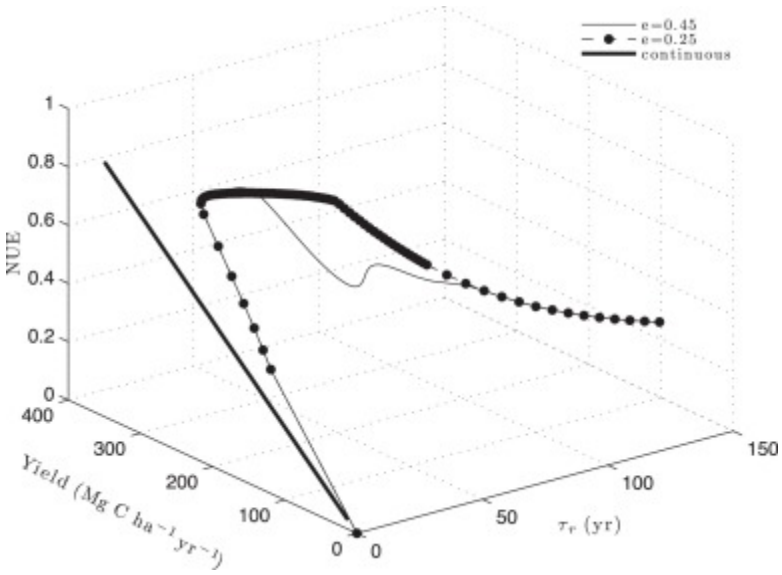

Fig. 11. Ecosystem N use efficiency for continuous and rotational harvest systems as a function of the average yield and heterotrophic carbon use efficiency (*e*). $(C/N)_{hv} = (C/N)_p$, $a = 0$, and other parameters are listed in Table 1. f_{hv} and τ_r are varied to obtain the yield gradients for continuous and rotational systems, respectively.

The emergence of the optimal rotation length and associated yield and *NUE* is related to the occurrence of net immobilization. Systems with a high degree of N limitation (i.e., high *e*) immobilize a relatively large amount of mineral N near the optimal rotation length (Fig. 10, Fig. 11). The effect of such intermittent immobilization is to retain N for later plant uptake. In comparison to the continuous model, where net mineralization always occurs, periodic immobilization in rotational systems results in a higher *NUE* for the same yield. Therefore, the non-linear dynamics resulting from strong plant–soil feedback induced by N limitation alter the relationship between yield and *NUE* in the modeled ecosystems.

5. Discussion and conclusions

Neglecting economic factors, the rotation length that maximizes biomass yield has been traditionally identified at the time of maximum annual increment (MAI), or the standing biomass normalized by the rotation length (e.g., Gregory, 1987). More recently, Dewar and McMurtrie, 1996a, Dewar and McMurtrie, 1996b linked the MAI concept to the soil N cycle in a steady-state analysis, assuming a constant and positive net mineralization rate. In contrast, Aber et al. (1982) found a monotonic yield increase with rotation length using a linear, donor-controlled decomposition and mineralization scheme. The dynamic and flexible MIT-DIR soil C–N cycling scheme used here demonstrated that soil mineral N cycling may alternate between net mineralization and net immobilization conditions during the rotation. Further, maximum N retention via decomposer immobilization was associated with the predicted optimal rotation length.

N retention by soil microbial communities has been observed to control post-harvest N availability and may be manipulated to improve *NUE* in harvested ecosystems. Vitousek and Matson (1985) noted that two years after harvest, plots where organic residue was left on site immobilized over 20% more N than plots with residual removal and herbicide application. In another study, long-term N fertilization over 8 years reduced microbial biomass and net mineralization, and increased gross immobilization, however litter removal had no effect (Fisk and Fahey, 2001). In the first year after clear-cut in a northern hardwood forest, gross mineralization, gross immobilization, and net mineralization increased, while microbial biomass remained the same, suggesting faster microbial N turnover after harvest (Holmes and Zak, 1999). These results suggest the microbial biomass dynamics are an important intermediary between fertilizer or residue application and plant N availability and there may be interactive effects between microbial C and N availability.

Our comparison of decomposition model structure illuminated potential opportunities for further study of factors leading to nonlinear transients in soil biogeochemical cycles. The multiplicative model was previously shown to reproduce oscillatory SOM-decomposer dynamics (Manzoni and Porporato, 2007). In the present study, both the multiplicative and Michaelis–Menten models predict soil C storage in litter and humus pools to be independent of the harvest strategy at long times, consistent with previous experimental results that showed soil C recovery over time after harvest (Covington, 1981, Richter et al., 1999, Yanai et al., 2003, Nave et al., 2010). In contrast, the linear model predicts decreased soil C storage in litter and humus with harvest, through a dependence on plant C storage and the fraction of harvested litter returned to the soil pool. In all models, the soil microbial biomass pool decreases with harvest and increases with residual application. Experimental and modeling evidence suggests chronic N addition increases soil C storage by reducing decomposition (Frey et al., 2014) or respiration (Sampson et al., 2006). Again, through its dependence on plant C storage, the linear model is the only model that predicts increased soil C storage with fertilization. However, neither model captures the corresponding changes in decomposition and respiration rate. All models predict a decrease in soil microbial biomass with harvest, consistent with experimental results (Holden and Treseder, 2014), and an increase with N fertilization. The predicted increase of soil microbial biomass with N fertilization contrasts recent experimental results, which suggest a complex response involving both substrate and microbial activity (Sampson et al., 2006, Treseder, 2008, Janssens et al., 2010, Frey et al., 2014). Modeling the response of soil C storage to harvest and fertilization therefore remains an important and outstanding research area.

Results from the continuously-harvested and clear-cut rotational ecosystem models provide insight into the differences between partial harvesting and clear-cut techniques. For the same yield, clear-cut systems exhibit greater *NUE* and mineralize more N than continuously-harvested systems (Fig. 4, Fig. 11). This is presumably due to the immobilization effect discussed above, as immobilization effectively

protects N from being lost from the mineral pool, by assimilation into litter and later release via mineralization for plant uptake. On the other hand, continuously-harvested systems always mineralize N, releasing it into the mineral N pool where it is susceptible to leaching losses. While there is little observational evidence to support this modeling result, one study observed a substantial decline in net N mineralization (approx. 50–70%) at mid-rotation, 15 years after harvest, whereas net N mineralization increased in control plots (Piatek and Allen, 1999). Finally, despite lower average losses, clear-cut systems exhibit large fluctuations in leaching rates (Fig. 4, Fig. 8), which may impact the chemistry of receiving waters (Scheffer and Carpenter, 2003, Leong et al., 2014).

Further analysis of the simplifying assumptions employed here may improve understanding of soil nitrogen mineralization-immobilization processes in harvested ecosystems. In particular, the assumption of constant C:N for plant, humus, and decomposer pools effectively lumps the carbon and nitrogen pools for these system components into a single state variable and thereby constrains the resulting dynamics. For example, tree C:N ratio may increase with age, as the fraction of woody biomass increases, or decrease with external fertilizer N input (Zhang and Allen, 1996), which may impose corresponding changes in litter N production over a rotation period. Simulations demonstrate that this assumption does not qualitatively alter our results (data not shown).

While hydro-climatic fluctuations and their resulting effects on soil hydrological processes were not explicitly modeled here, it is well-recognized that forest management alters the water balance with potential consequences for soil N cycling. Harvesting enhances leaching and runoff losses (Brown et al., 2005, Tian et al., 2012) and may increase the soil mineral N pool (Prescott, 1997), which both contribute to increased N export. All models considered here predict an increase in soil mineral N and, therefore leaching, with both fertilization and harvest. However, from a hydrological perspective, our model likely under-predicts the sensitivity of N leaching to harvest because it only includes this effect on the soil mineral N pool. In addition, we note that N may be exported as organic or inorganic and the relative amounts of each may depend on the intensity of management activities (Perakis and Hedin, 2002). We conducted simulations with the leaching flux transferred to the organic N pools and found that the main conclusions were not qualitatively affected.

The model used in this paper exhibits a wide range of dynamical behaviors that depend on the harvest strategy and N fertilization regime. Interestingly, the strength of plant–soil feedback was shown to have an impact on soil mineralization-immobilization and its feedback to biomass yield. The results suggest ecosystem function under rotational harvest, specifically N retention and *NUE*, can be optimized via the mineralization-immobilization regime. The prospect of variable soil biogeochemical cycling regimes through time raises further questions related to the optimal timing of fertilizer or lime additions and the interaction of soil hydrology and biogeochemistry in rainfed and irrigated systems.

Acknowledgments

The authors thank G. Katul and D.DeB. Richter for helpful discussions and comments and acknowledge support from the U.S. Department of Energy (DOE) through the Office of Biological and Environmental Research (BER) Terrestrial Carbon Processes (TCP) program (DE-SC0006967); the National Science Foundation (DGE-1068871, NSF-EAR-0838301, NSF-EAR-1331846, and NSF-EAR-1316258); and the United States Department of Agriculture through the Agriculture and Food Research Initiative (2011-67003-30222). We acknowledge the thoughtful comments of two anonymous reviewers.

References

Aber et al., 1982. J.D. Aber, J.M. Melillo, C.A. Federer. **Predicting the effects of rotation length, harvest intensity, and fertilization on fiber yield from northern hardwood forests in New England.** *For. Sci.,* 28 (1982), pp. 31-45

Bolker et al., 1998. B.M. Bolker, S.W. Pacala, W.J. Parton Jr. **Linear analysis of soil decomposition: insights from the century model.** *Ecol. Appl.,* 8 (1998), pp. 425-439

Brady and Weil, 2004. N.C. Brady, R.R. Weil. **The Nature and Properties of Soils.** (13th ed.), Prentice Hall, Upper Saddle River, NJ (2004)

Brown et al., 2005. A.E. Brown, L. Zhang, T.A. McMahon, A.W. Western, R.A. Vertessy. **A review of paired catchment studies for determining changes in water yield resulting from alterations in vegetation.** *J. Hydrol*., 310 (2005), pp. 28-61

Canham et al., 2013. C.D. Canham, N. Rogers, T. Buchholz. **Regional variation in forest harvest regimes in the northeastern United States.** *Ecol. Appl*., 23 (2013), pp. 515-522

Corbeels et al., 2005.
M. Corbeels, R.E. McMurtrie, D.A. Pepper, D.S. Mendham, T.S. Grove, A.M. O'Connell. **Long-term changes in productivity of eucalypt plantations under different harvest residue and nitrogen management practices: a modelling analysis.** *For. Ecol. Manag*., 217 (2005), pp. 1-18

Covington, 1981. W.W. Covington. **Changes in forest floor organic matter and nutrient content following clear cutting in northern hardwoods.** *Ecology*, 62 (1981), pp. 41-48

Dangal et al., 2014. S.R.S. Dangal, B.S. Felzer, M.D. Hurteau. **Effects of agriculture and timber harvest on carbon sequestration in the eastern US forests.** *J.* Geophys. Res. Biogeosci., 119 (2014), pp. 35-54

Dewar and McMurtrie, 1996a. R.C. Dewar, R.E. McMurtrie. **Analytical model of stemwood growth in relation to nitrogen supply.** *Tree Physiol*., 16 (1996), pp. 161-171

Dewar and McMurtrie, 1996b. R.C. Dewar, R.E. McMurtrie. **Sustainable stemwood yield in relation to nitrogen balance of forest plantations: a model analysis.** *Tree Physiol*., 16 (1996), pp. 173-182

D'odorico et al., 2003. P. D'odorico, F. Laio, A. Porporato, I. Rodriguez-Iturbe. **Hydrologic controls on soil carbon and nitrogen cycles. II. A case study.** *Adv. Water Resour*., 26 (1) (2003), pp. 59-70

Fisk and Fahey, 2001. M.C. Fisk, T.J. Fahey. **Microbial biomass and nitrogen cycling responses to fertilization and litter removal in young northern hardwood forests.** *Biogeochemistry*, 53 (2001), pp. 201-223

Frey et al., 2014.
S.D. Frey, S. Ollinger, K. Nadelhoffer, R. Bowden, E. Brzostek, A. Burton, B.A. Caldwell, S.Crow, C. L. Goodale, A.S. Grandy, A. Finzi, M.G. Kramer, K. Lajtha, J. LeMoine, M. Martin, W.H.McDowell, R. Minocha, J.J. Sadowsky, P.H. Templer, K. Wickings. **Chronic nitrogen additions suppress decomposition and sequester soil carbon in temperate forests.** *Biogeochemistry*, 121 (2014), pp. 305-316

Goulding et al., 2008. K. Goulding, S. Jarvis, A. Whitmore. **Optimizing nutrient management for farm systems.** *Philos. Trans. R. Soc. B*, 363 (2008), pp. 667-680

Gregory, 1987. G.R. Gregory. **Resource Economics for Foresters.** John Wiley and Sons, Somerset, NJ (1987)

Guo and Gifford, 2002. L.B. Guo, R.M. Gifford. **Soil carbon stocks and land use change: a meta-analysis.** *Glob. Change Biol.*, 8 (2002), pp. 345-360

Holden and Treseder, 2014. S.R. Holden, K.K. Treseder. **A meta-analysis of soil microbial biomass responses to forest disturbances.** *Microb. Regul. Glob. Biogeochem. Cycles*, 88 (2014)

Holmes and Zak, 1999. W.E. Holmes, D.R. Zak. **Soil microbial control of nitrogen loss following clear-cut harvest in northern hardwood ecosystems.** *Ecol. Appl.*, 9 (1999), pp. 202-215

Janssens et al., 2010.
I.A. Janssens, W. Dieleman, S. Luyssaert, J.A. Subke, M. Reichstein, R. Ceulemans, P.Ciais, A.J. Do lman, J. Grace, G. Matteucci, D. Papale. **Reduction of forest soil respiration in response to nitrogen deposition.** *Nat. Geosci.*, 3 (2010), pp. 315-322

Jerabkova et al., 2011. L. Jerabkova, C.E. Prescott, B.D. Titus, G.D. Hope, M.B. Walters. **A meta-analysis of the effects of clearcut and variable-retention harvesting on soil nitrogen fluxes in boreal and temperate forests.** *Can. J. For. Res.*, 41 (2011), pp. 1852-1870

Johnson, 1992. D.W. Johnson. **Effects of forest management on soil carbon storage.** *Water Air Soil Pollut.*, 64 (1992), pp. 83-120

Johnson and Curtis, 2001. D.W. Johnson, P.S. Curtis. **Effects of forest management on soil C and N storage: meta analysis.** *For. Ecol. Manag.*, 140 (2001), pp. 227-238

Jorgensen et al., 1980. J.R. Jorgensen, C.G. Wells, L.J. Metz. **Nutrient changes in decomposing loblolly pine forest floor.** *Soil Sci. Soc. Am. J.*, 44 (1980), pp. 1307-1314

Leong et al., 2014. D.N.S. Leong, S.D. Donner, M.A. Hassan, R. Gabor, J.D. Drummond. **Sensitivity of stoichiometric ratios in the Mississippi River to hydrologic variability.** *J. Geophys. Res. Biogeosci.*, 119 (2014), pp. 1049-1062

Manzoni and Porporato, 2007. S. Manzoni, A. Porporato. **A theoretical analysis of nonlinearities and feedbacks in soil carbon and nitrogen cycles.** *Soil Biol. Biochem.*, 39 (2007), pp. 1542-1556

Manzoni and Porporato, 2009. S. Manzoni, A. Porporato. **Soil carbon and nitrogen mineralization: theory and models across scales.** *Soil Biol. Biochem.*, 41 (2009), pp. 1355-1379

Mobley, 2011. M.L. Mobley. *An Ecosystem Approach to Dead Plant Carbon over 50 years of Old-Field Forest.* (PhD Thesis). Duke University (2011)

Mobley et al., 2013. M.L. Mobley, D.DeB. Richter, P.R. Heine. **Accumulation and decay of woody detritus in a humid subtropical secondary pine forest.** *Can. J. For. Res.*, 43 (2013), pp. 109-118

Mobley et al., 2015. M.L. Mobley, K. Lajtha, M.G. Kramer, A.R. Bacon, P.R. Heine, D.D. Richter. **Surficial gains and subsoil losses of soil carbon and nitrogen during secondary forest development.** *Glob. Change Biol*., 21 (2015), pp. 986-996

Murray, 2002. J.D. Murray. **Mathematical Biology: An Introduction.** (3rd ed.), Springer, New York, NY (2002)

Nave et al., 2010. L.E. Nave, E.D. Vance, C.W. Swanston, P.S. Curtis. **Harvest impacts on soil carbon storage in temperate forests.** *For. Ecol. Manag*., 259 (2010), pp. 857-866

Peckham et al., 2013. S.D. Peckham, S.T. Gower, C.H. Perry, B.T. Wilson, K.M. Stueve. **Modeling harvest and biomass removal effects on the forest carbon balance of the Midwest, USA.** *Environ. Sci. Policy*, 25 (2013), pp. 22-35

Peng et al., 2002. C. Peng, H. Jiang, M.J. Apps, Y. Zhang. **Effects of harvesting regimes on carbon and nitrogen dynamics of boreal forests in central Canada: a process model simulation.** *Ecol. Model*., 155 (2002), pp. 177-189

Perakis and Hedin, 2002. S.S. Perakis, L.O. Hedin. **Nitrogen loss from unpolluted South American forests mainly via dissolved organic compounds.** *Nature*, 415 (2002), pp. 416-419

Piatek and Allen, 1999. K.B. Piatek, H.L. Allen. **Nitrogen mineralization in a pine plantation fifteen years after harvesting and site preparation.** *Soil Sci. Soc. Am. J*., 63 (1999), pp. 990-998

Porporato and Rodriguez-Iturbe, 2013. A. Porporato, I. Rodriguez-Iturbe. **From random variability to ordered structures: a search for general synthesis in ecohydrology.** *Ecohydrology*, 6 (2013), pp. 333-342

Porporato et al., 2003. A. Porporato, P. D'Odorico, F. Laio, I. Rodriguez-Iturbe. **Hydrologic controls on soil carbon and nitrogen cycles. I. Modeling scheme.** *Adv. Water Resour*., 26 (2003), pp. 45-58

Porporato et al., 2015. A. Porporato, X. Feng, S. Manzoni, Y. Mau, A.J. Parolari, G. Vico. **Ecohydrological modeling in agroecosystems: examples and challenges.** *Water Resour. Res*., 51 (2015), pp. 5081-5099

Prescott, 1997. C.E. Prescott. **Effects of clearcutting and alternative silvicultural systems on rates of decomposition and nitrogen mineralization in coastal montane coniferous forest.** *For. Ecol. Manag*., 95 (1997), pp. 253-260

Richter and Markewitz, 1995. D.D. Richter, D. Markewitz. **Atmospheric deposition and soil resources of the southern pine forest.** S. Fox, R. Mikler (Eds.), Impact of Air Pollutants on Southern Pine Forests, Springer, New York (1995)

Richter et al., 1999. D.D. Richter, D. Markewitz, S.E. Trumbore, C.G. Wells. **Rapid accumulation and turnover of soil carbon in a re-establishing forest.** *Nature*, 400 (1999), pp. 56-58

Richter et al., 2000. D.D. Richter, D. Markewitz, P.R. Heine, V. Jin, J. Raikes, K. Tian, C.G. Wells. **Legacies of agriculture and forest regrowth in the nitrogen of old-field soils.** *For. Ecol. Manag*., 138 (2000), pp. 233-248

Rolff and Agren, 1999. C. Rolff, G.I. Agren. **Predicting effects of different harvesting intensities with a model of nitrogen limited forest growth.** *Ecol. Model*., 118 (1999), pp. 193-211

Sampson et al., 2006. D.A. Sampson, R.H. Waring, C.A. Maier, C.M. Gough, M.J. Ducey, K.H. Johnsen. **Fertilization effects on forest carbon storage and exchange, and net primary production: a new hybrid process model for stand management.** *For. Ecol. Manag*., 221 (2006), pp. 91-109

Scheffer and Carpenter, 2003. M. Scheffer, S.R. Carpenter. **Catastrophic regime shifts in ecosystems: linking theory to observation.** *Trends Ecol. Evol*., 18 (2003), pp. 648-656

Schimel and Bennett, 2004. J.P. Schimel, J. Bennett. **Nitrogen mineralization: challenges of changing paradigm.** *Ecology*, 85 (2004), pp. 591-602

Shcherbak et al., 2014. L. Shcherbak, N. Millar, G.P. Robertson. **Global metaanalysis of the nonlinear response of soil nitrous oxide (N_2O) emissions to fertilizer nitrogen.** *Proc. Natl. Acad. Sci. U. S. A.,* 111 (2014), pp. 9199-9204

Smith et al., 1997. D.M. Smith, B.C. Larson, M.J. Kelty, P.M.S. Ashton. **The Practice of Silviculture: Applied Forest Ecology.** (9th ed.), Wiley, New York (1997)

Thornley and Cannell, 2000. J.H.M. Thornley, M.G.R. Cannell. **Managing forests for wood yield and carbon storage: a theoretical study.** *Tree Physiol*., 20 (2000), pp. 477-484

Tian et al., 2012. S. Tian, M.A. Youssef, R.W. Skaggs, D.M. Amatya, G.M. Chescheir. **Modeling water, carbon, and nitrogen dynamics for two drained pine plantations under intensive management practices.** *For. Ecol. Manag*., 264 (2012), pp. 20-36

Treseder, 2008. K.K. Treseder. **Nitrogen additions and microbial biomass: a meta-analysis of ecosystem studies.** *Ecol. Lett*., 11 (2008), pp. 1111-1120

Vergutz et al., 2012. L. Vergutz, S. Manzoni, A. Porporato, R. Ferreira Novais, R.B. Jackson. **Global resorption efficiencies and concentrations of carbon and nutrients in leaves of terrestrial plants.** *Ecol. Monogr*., 82 (2012), pp. 205-220

Vitousek and Matson, 1985. P.M. Vitousek, P.A. Matson. **Disturbance, nitrogen availability, and nitrogen losses in an intensively managed loblolly pine plantation.** *Ecology*, 66 (1985), pp. 1360-1376

Wang et al., 2014.
F. Wang, D.J. Mladenoff, J.A. Forrester, J.A. Blanco, R.M. Scheller, S.D. Peckham, C. Keough, M.S . Lucash, S.T. Gower. **Multimodel simulations of forest harvesting effects on long-term productivity and CN cycling in aspen forests.** *Ecol. Appl*., 24 (2014), pp. 1374-1389

Wei et al., 2003. X. Wei, J.P. Kimmins, G. Zhou. **Disturbances and the sustainability of long-term site productivity in lodgepole pine forests in the central interior of British Columbia – an ecosystem modeling approach.** *Ecol. Model*., 164 (2003), pp. 239-256

Williams et al., 2012. C.A. Williams, G.J. Collatz, J. Masek, S.N. Goward. **Carbon consequences of forest disturbance and recovery across the conterminous United States.** *Glob. Biogeochem. Cycles*, 26 (1) (2012)

Xu et al., 2013. X. Xu, P.E. Thornton, W.M. Post. **A global analysis of soil microbial biomass carbon, nitrogen, and phosphorus in terrestrial ecosystems.** *Glob. Ecol. Biogeogr*., 22 (2013), pp. 737-749

Yanai et al., 2003. R.D. Yanai, W.S. Currie, C.L. Goodale. **Soil carbon dynamics after forest harvest: an ecosystem paradigm reconsidered.** *Ecosystems*, 6 (2003), pp. 197-212

Zelenev et al., 2005. V.V. Zelenev, A.H.C. van Bruggen, A.M. Semenov. **Short-term wavelike dynamics of bacterial populations in response to nutrient input from fresh plant residues.** *Microb. Ecol*., 49 (2005), pp. 83-93

Zhang and Allen, 1996. S. Zhang, H.L. Allen. **Foliar nutrient dynamics of 11-year-old loblolly pine (*Pinus taeda*) following nitrogen fertilization.** *Can. J. For. Res*., 26 (1996), pp. 1426-1439